



Revista UIS Ingenierías

ISSN: 1657-4583

ISSN: 2145-8456

revistaingenierias@uis.edu.co

Universidad Industrial de Santander

Colombia

Franco-Rendón, Carlos Mauricio; León-Henao, Henry; Bedoya-Zapata, Álvaro Diego; Santa, Juan Felipe; Giraldo B., Jorge Enrique

Failure analysis of fillet welds with premature corrosion in 316L stainless steel slide gates using constitution diagrams

Revista UIS Ingenierías, vol. 19, núm. 2, 2020, -Junio, pp. 141-148

Universidad Industrial de Santander

Bucaramanga, Colombia

DOI: <https://doi.org/10.18273/revuin.v19n2-2020016>

Disponible en: <https://www.redalyc.org/articulo.oa?id=553768132016>

- Cómo citar el artículo
- Número completo
- Más información del artículo
- Página de la revista en redalyc.org

redalyc.org

Sistema de Información Científica Redalyc

Red de Revistas Científicas de América Latina y el Caribe, España y Portugal

Proyecto académico sin fines de lucro, desarrollado bajo la iniciativa de acceso abierto

# Failure analysis of fillet welds with premature corrosion in 316L stainless steel slide gates using constitution diagrams

## Análisis de falla de soldaduras en filete con corrosión prematura en compuertas deslizantes de acero inoxidable 316L usando diagramas de constitución

Carlos Mauricio Franco-Rendón <sup>1a</sup>, Henry León-Henao <sup>1b</sup>, Álvaro Diego Bedoya-Zapata <sup>1c</sup>,  
Juan Felipe Santa <sup>2</sup>, Jorge Enrique Giraldo B. <sup>3</sup>

<sup>1</sup> Grupo de Soldadura, Ingeniería Mecánica, Universidad Nacional de Colombia, Colombia.  
Orcid: <sup>a</sup> 0000-0001-9003-5255, <sup>b</sup> 0000-0002-5557-2060 Emails: <sup>a</sup> cmfrancor@unal.edu.co, <sup>b</sup> hleonh@unal.edu.co,  
<sup>c</sup> adbedoyaz@unal.edu.co

<sup>2</sup> Grupo de Investigación Materiales Avanzados y Energía (MATyER), Instituto Tecnológico Metropolitano, Colombia. Email: jfsanta@gmail.com

<sup>3</sup> Grupo de Soldadura, Departamento de Materiales, Universidad Nacional de Colombia, Colombia.  
Orcid: 0000-0001-6614-0661, Email: jegirald@unal.edu.co

Received: 16 December 2019. Accepted: 28 January 2020. Final version: 25 March 2020.

### Abstract

The service environment of the slide gates may cause localized corrosion at welds. In this work, a failure analysis was conducted to determine the causes of the premature corrosion of the fillet welds before the commissioning. According to the contractor, the slide gates were manufactured in ASTM A240 Type 316L stainless steel and welded with GMAW using an ER316LSi filler metal. Test samples of the fillet weld metals were extracted from gates after a preliminary visual inspection. The samples were analyzed using ferrite number measurements, Optical Emission Spectrometry, chemical analysis, metallographic examination and Scanning Electron Microscopy with microanalysis. The analysis of results using the Schaeffler and WRC-92 constitution diagrams showed that the estimated chemical composition of the filler metal differs with the filler metal specified in the WPS suggesting that an incorrect carbon steel filler metal was used during the construction of the gates.

**Keywords:** corrosion; stainless steel; filler metal selection; Schaeffler diagram; WRC-1992 diagram; slide gate.

### Resumen

Las condiciones de servicio de compuertas deslizantes en una planta de tratamiento de aguas residuales pueden causar corrosión localizada en las soldaduras. Se realizó un análisis de falla para determinar las causas de corrosión prematura en las soldaduras en filete de varias compuertas antes de su servicio. El contratista de las compuertas afirmó que las fabricó en acero inoxidable ASTM A240 Tipo 316L y las soldó con proceso GMAW y electrodo ER316LSi. Después de una inspección visual, se extrajeron dos muestras de metales fundidos de las compuertas y se analizaron utilizando medición de ferrita, espectrometría de emisión óptica, análisis químico, examen metalográfico y SEM con microanálisis. El análisis, usando los diagramas de Schaeffler y WRC-92, mostró que la composición química estimada para el metal de aporte difiere de la reportada en el WPS, sugiriendo que durante la construcción de las compuertas se usó un electrodo incorrecto de acero al carbono.

**Palabras clave:** corrosión; acero inoxidable; selección de material de aporte; diagrama de Schaeffler; diagrama WRC-1992; compuerta deslizante.

## 1. Introducción

Corrosion is a major issue industrially. The global cost of corrosion is estimated to be US\$2.5 trillion in 2013 [1]. Every year, millions of dollars are lost by improper materials selection and subsequently corrosion. Storage tanks and piping systems used for water treatment are typically manufactured in stainless steels [2]; [3] to avoid corrosion. Slide gates used in water treatment plants are also manufactured in stainless steel in order to avoid corrosion during the service. The gate panel is usually conformed by a flat plate reinforced with several stiffeners joined by fillet or groove welds. Typical materials used for plates and stiffeners belong to series 3XX austenitic stainless steels grade such as grades 304, 304L, 316, 316L, since they have good weldability and corrosion resistance in moderated service conditions. In fact, these four alloys are the materials required for the American Water Works Association to build slide gates according to the paragraph 4.3.3.1 of the standard ANSI/AWWA C561-04 “Fabricated Stainless Steel Slide Gates” [4]. The filler metals used commonly to do the joint welds in stainless steel gates have similar chemical composition of base metals. A few examples of filler metals specified for GMAW and GTAW welding processes are ER308L, ER308MoL, ER309L, ER309MoL, ER316, ER316L, ER316LSi, ER316L among others included in the Table 3.3 of the AWS D1.6 “Structural Welding Code –Stainless Steel” [5] which is the code that must be met for welded slide gates according to the AWWA C561, paragraph 4.5.2.1 [4]. All these filler metals are classifications given in standard AWS A5.9 [6].

This paper reports the failure analysis conducted to determine the causes of the accelerated corrosion of the fillet welds used to join the stiffeners and appurtenances of several slide gates from a water treatment plant before the commissioning. These gates were manufactured using austenitic stainless steel grade 316L under ASTM A240 standard [7] and, according to the manufacturer’s WPS, welded with GMAW using ER316LSi filler metal. The weld metals of these fillet welds shown surface corrosion and some pitting during the field assembly much before the actual service, moreover, these joints had an unexpected ferromagnetic behavior in this kind of material (grade 316L). Figure 1 shows numerous indications of corrosion in the welded joints.

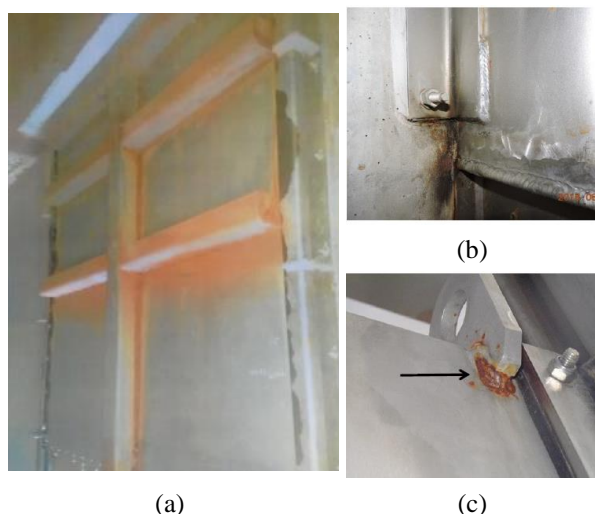


Figure 1. Indication of corrosion at welds in slide gates of the water treatment plant: (a) General corrosion in the slide gates stiffeners, (b) Corrosion at fillet welds and (c) Corrosion at fillet weld in lifting lugs.

## 2. Experimental

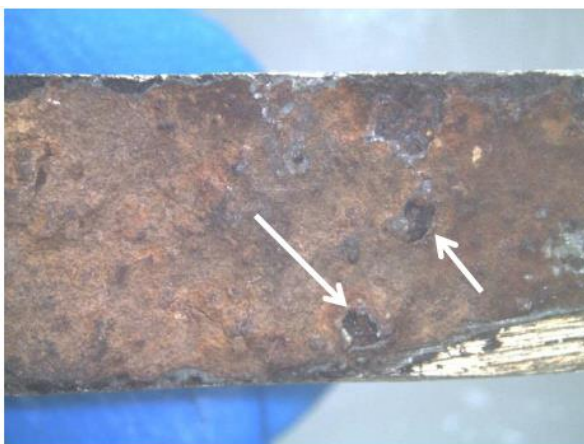
After a preliminary field inspection, two samples of weld metals were extracted from fillet welds of two different slide gates just in the joint plate-stiffener. These two specimens were called sample #1 and sample #2 (Figure 2). The weld metal samples have around 60-63 mm of length. Using the samples extracted for the analysis, a visual and stereoscopic inspection was done.

The chemical composition of base and weld metals was measured using optical emission spectrometry (OES) in a Bruker Q8 Magellan equipment. The ferrite number of the weld metals was measured with a Magne Gage equipment. The transverse sections of the board-stiffener joints samples were prepared in Bakelite, polished using sand paper and polished for metallography with alumina particles of 12.5  $\mu\text{m}$  and diamond 1  $\mu\text{m}$ . The samples were etched using Nital 2 (110 ml of ethyl alcohol + 2 ml of nitric acid). The microstructure of both weld metals was analyzed using optical microscopy in a NIKON Eclipse optical microscope. The hardness of the samples was measured in a DiaTestor 2Rc durometer manufactured by Otto Wolpert-Werke with 30 kgf load. The rust layers on the samples were evaluated using Scanning of Electron Microscopy (SEM) using a JEOL JSM7100F microscope with an EDS Oxford analyzer and they were coated with gold using a sputtering system. Both samples (# 1 and # 2) were inspected in the SEM.

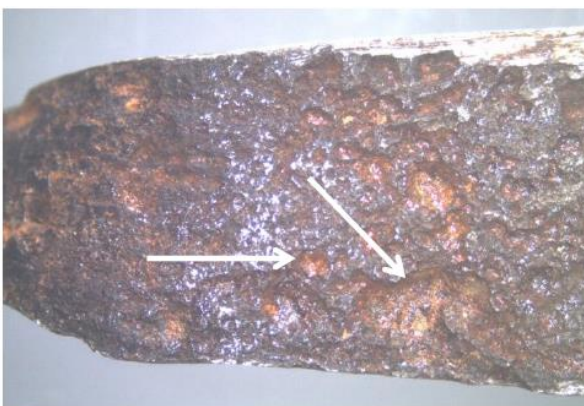
### 3. Results and discussion

#### 3.1. Visual inspection

Figure 2 shows the surface condition of the samples using a stereomicroscope. The general corrosion and pitting of the surface over sample #1 (Figure 2 (a)) is evident. Figure 2 (b) shows the surface of sample #2: in this case, it has general corrosion too and the pits are also evident as observed for sample #1. The pits in both samples are indicated by the arrows.



(a)



(b)

Figure 2. General corrosion and pitting presented in the samples: (a) Sample #1 and (b) Sample #2.

#### 3.2. Ferrite number and chemical composition

Both samples of weld metals showed a high ferromagnetic attraction. It was not possible to measure the ferrite number with the Magne Gage because the ferromagnetic attraction exceeded the maximum limit of the equipment indicating FN values greater than 80,

which is extremely high for austenitic stainless steels weld metals.

The chemical composition of both samples was determined, each one representing a different fillet weld metal. The chemical composition of weld metal is a mixture resulting from the base metal (316L) and the filler metal used during the manufacturing (unknown). Table 1 shows the results of chemical composition obtained in OES for both samples and the chemical composition requirements established in standards ASTM A240 Type 316L (base metal) and AWS A5.9 Classification ER319LSi (filler metal) [6] [7].

Considering that in a fusion welding process the weld metal is a mixture of base metal and filler metal, then the weld metal must have a chemical composition ranging between the alloying elements of filler and base metal [8]. In this case, the chromium content varied from 3.159% and 3.658% despite was expected a minimum value above and near 16% considering the mixture of 316L-ER316LSi. Accordingly, the resulting chemical composition of the weld metals cannot be considered as “stainless steels” since its chromium contents has to be higher than 10.5% [9]. The nickel content was extremely low: 3.19 and 3.658% for samples #1 and #2 respectively. If the 316L stiffener would have been welded with ER316LSi the nickel content should have been higher than 10% and lower than 14%.

Molybdenum is added to some stainless steels like 316L in order to increase its pitting resistance [10]. If an ASTM A240 type 316L steel had been welded with an ER316LSi filler metal, molybdenum contents of the weld metal should have been between 2 – 3%. In this case, the actual contents of molybdenum are 0.138 and 0.401% for sample 1 and 2, respectively, which is very low. Finally, low carbon stainless steels (denominated with “L”) had carbon contents under 0.03%, but the fillet weld metals studied have carbon contents of 0.06% and 0.053% for sample #1 and #2, respectively, which doubles the maximum limit of 0.03%. The analysis indicates that the filler metal used during the sliding gates manufacturing was not the class ER316LSi nor any other included in AWS A5.9 standard suitable to weld 316L metal (like ER316L, ER316, ER316LSi or ER316LMn).

#### 3.3. Microstructural and hardness analysis

The microstructure and average hardness of each sample is shown in Figure 3.



Table 1. Results of chemical composition for samples #1 and #2 and limits according to standards

| ALLOY ELEMENT<br>(SYMBOL) | ALLOY CONTENT (%) |           | STANDARDS REQUIREMENTS (%) |                            |
|---------------------------|-------------------|-----------|----------------------------|----------------------------|
|                           | SAMPLE #1         | SAMPLE #2 | ASTM A240<br>TP 316L       | AWS A5.9<br>CLASS ER316LSi |
| Carbon (C)                | 0.060             | 0.053     | 0.030 Max                  | 0.030 Max                  |
| Chromium (Cr)             | 3.159             | 3.658     | 16 - 18                    | 18 - 20                    |
| Nickel (Ni)               | 1.384             | 1.795     | 10 - 14                    | 11 - 14                    |
| Molybdenum (Mo)           | 0.138             | 0.401     | 2 - 3                      | 2 - 3                      |
| Manganese (Mn)            | 1.408             | 1.436     | 2                          | 1 - 2.5                    |
| Silicon (Si)              | 0.788             | 0.763     | 0.75                       | 0.65 - 1                   |
| Phosphorus (P)            | 0.016             | 0.017     | -                          | 0.03 Max.                  |
| Sulfur (S)                | 0.014             | 0.012     | -                          | 0.03 Max.                  |
| Niobium (Nb)              | 0.014             | 0.016     | NS                         | NS                         |
| Nitrogen (N)              | 0.04              | 0.04      | 0.1                        | NS                         |
| Copper (Cu)               | 0.127             | 0.132     | NS                         | 0.75 Max                   |

The microstructure of sample #1 (Figure 3 (a)) consists in ferrite with non – aligned second phase (FS(NA)) and polygonal ferrite islands (PF). Figure 3 (b) shows the microstructure and average hardness for sample #2: it also consists of several forms of ferrite including polygonal ferrite (PF), acicular ferrite (AF) and some regions with Widmanstätten ferrite. These microstructures have been reported by other authors for low carbon and low-alloy weld metals [11]. All these microstructures and phases are atypical for 316L-ER316LSi stainless steel welds which are mainly austenitic with little amounts of ferrite [9]. They are commonly found in high strength low alloy steels (HSLA) [12]. The results of microstructure analysis also indicated that the filler metal was not an ER316LSi.

Samples #1 and #2 have an average hardness of  $331 \pm 5$  HV and  $352 \pm 4.4$  HV respectively. These values of hardness are much higher than those expected for weld metals obtained with 316L base metal and ER316L filler metal which have values commonly between 150-160 HV. This unusual hardness levels indicated, again, that the welds were not obtained using ER316LSi filler metal.

### 3.4. SEM analysis

Corrosion at the samples was examined by SEM and the weld metals were analyzed using micro-analysis with Energy-Dispersive Spectrometry (EDS). Figure 4 shows the transverse section of samples analyzed in scanning electron microscope. In this Figure, a heavy rust layer (80-100  $\mu\text{m}$ ) can be seen on the surface of the samples (Figure 4(a)) and several pits onto the weld metal are also evident (Figures 4(a) and 4(b)).

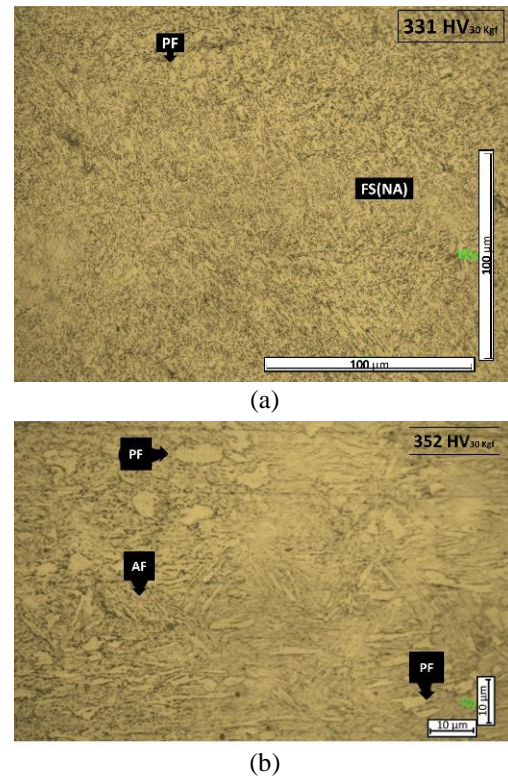


Figure 3. Microstructure and average hardness of: (a) Sample #1 - (b) Sample #2.

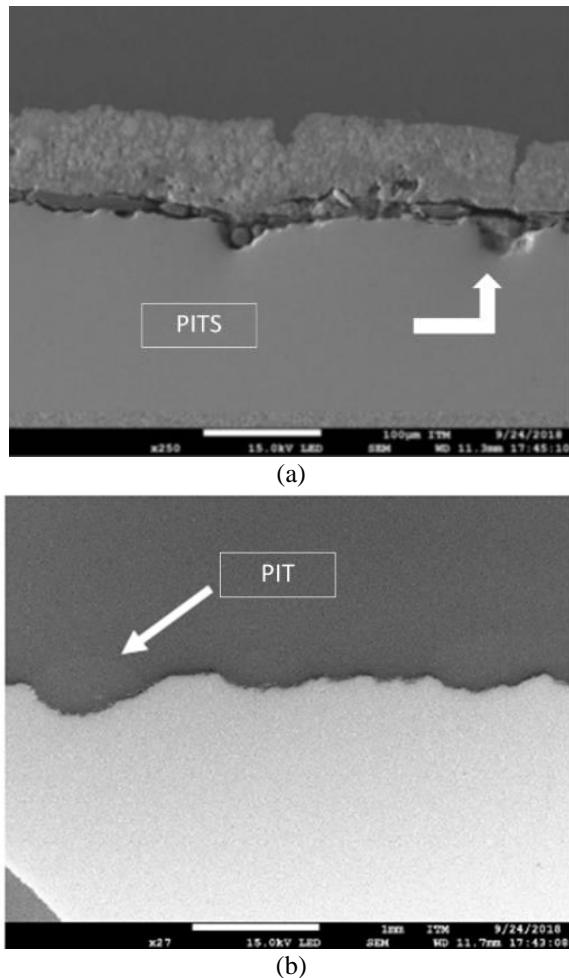


Figure 4. Transverse section of both samples in SEM: (a) Sample #1 and (b) Sample #2.

### 3.5. Problem synthesis using constitution diagrams

Both Schaeffler and WRC-92 constitution diagrams were used to establish the possible family of filler metals used in the welds. Table 2 summarizes the results of  $Cr_{eq}$  and  $Ni_{eq}$  calculated for both diagrams using the compositional values of samples #1 and #2 included in Table 1 and the averages of eleven Material Test Reports (MTRs) for the base metal type 316L provided by the manufacturer of the gates.

#### 3.5.1. Schaeffler diagram

The Schaeffler diagram was used to find the family of filler metals possibly used in shop to apply the fillet welds from where the samples were extracted, as shown in Figure 5. The Schaeffler diagram shows the base metal (BM) and the weld metals represented by the samples #1 and #2 (WM). The finding of the family of filler metals is based in the metallurgical fact that the line

$(Cr_{EQUIV}, Ni_{EQUIV})_{BASE METAL} - (Cr_{EQUIV}, Ni_{EQUIV})_{WELD METAL}$  points to the family of filler metals used to obtain the particular weld metal on the particular base metal [8]. The Figure 5 shows that the line  $(Cr_{EQUIV}, Ni_{EQUIV})_{BASE METAL} - (Cr_{EQUIV}, Ni_{EQUIV})_{WELD METAL}$  SAMPLES 1&2 points clearly to the family of carbon steel filler metals (yellow circle at the left down zone in the diagram), possibly the classifications included in AWS A5.1:2012 for SMAW [13] or AWS A5.18:2005 for GMAW/GTAW/PAW/SAW [14].

Table 2.  $Cr_{eq}$  and  $Ni_{eq}$  calculations for samples (#1 and #2) and base metal for use with the Schaeffler and WRC-92 diagrams

| MATERIAL          |     | SCHAEFFLER |           | WRC-92    |           |
|-------------------|-----|------------|-----------|-----------|-----------|
|                   |     | $Cr_{eq}$  | $Ni_{eq}$ | $Cr_{eq}$ | $Ni_{eq}$ |
| SAMPLES           | # 1 | 4.5        | 3.9       | 3.3       | 4.3       |
|                   | # 2 | 5.2        | 4.1       | 4.1       | 4.5       |
| BASE METAL (GATE) |     | 19.7       | 11.3      | 18.7      | 11.5      |

More than 25 classifications are included on AWS A5.1/A5.18 standards [13] [14], but they have no significant changes in  $Cr_{eq}$  and  $Ni_{eq}$ . Two of the most common electrodes were analyzed as candidates to perform a first approach to determine the possible filler metal used to build the gates: E7018 for SMAW process and ER70S-6 for the GMAW process. Table 3 summarizes the typical chemical composition given by several producers of filler metals for classes E7018/ER70S-6 and the calculations of  $Cr_{eq}$  and  $Ni_{eq}$ , as well as the averages [16] [17] [18].

The candidate filler metals (E7018 and ER70S-6) were located in the Schaeffler diagram (Figure 6) using their coordinates of  $Cr_{eq}$  and  $Ni_{eq}$  calculated with the chemical composition resumed in the Table 3, and the base and weld metals reported in Table 2. These filler metals are exactly in the line  $(Cr_{EQUIV}, Ni_{EQUIV})_{BASE METAL} - (Cr_{EQUIV}, Ni_{EQUIV})_{WELD METAL}$  SAMPLES 1&2 and the calculation of the dilution percentage (see formula above of the diagram) ranged from 22% to 23%, which is in agreement to the dilution values for fillet welds near to 20% reported in the literature [15].

#### 3.5.2. WRC-92 diagram

In a similar approach, the WRC-92 constitution diagram was used in order to verify the results obtained with Schaeffler diagram. Figure 7 shows the average gates base metal (BM), the pair of fillet weld metals (WM) and the average of different filler metals (FM) plotted in the WRC-92 diagram.

The same procedure used to locate the samples in the Schaeffler was carried out again for the WRC-92 diagram

and in this case the location of the filler metals falls, again, in the line connecting the base metal and the weld metals. The dilution percentage calculated it is around 20.1% and is according to fillet welds. In this case, the values are very similar to the dilution percentages obtained in the Schaeffler diagram and those reported in the literature [15].

### 3.6. General discusión

Microstructures of the gate's fillet weld metals composed by large amounts of different kinds of ferrite (acicular ferrite, polygonal ferrite and some regions with

Widmanstätten ferrite) so different to austenitic stainless steel weld metals, excessive high values of hardness (331-352 HV) compared with ordinary hardness in austenitic stainless steel weld metals (150-160 HV) and chemical composition with low levels of chromium (3.159-3.658%), nickel (1.384-1.795%), molybdenum (0.138-0.401%), and high carbon (0.053-0.060%), allows to affirm that the corroded welds in the gate were no applied with ER316LSi as the contractor affirm in your WPS and records.

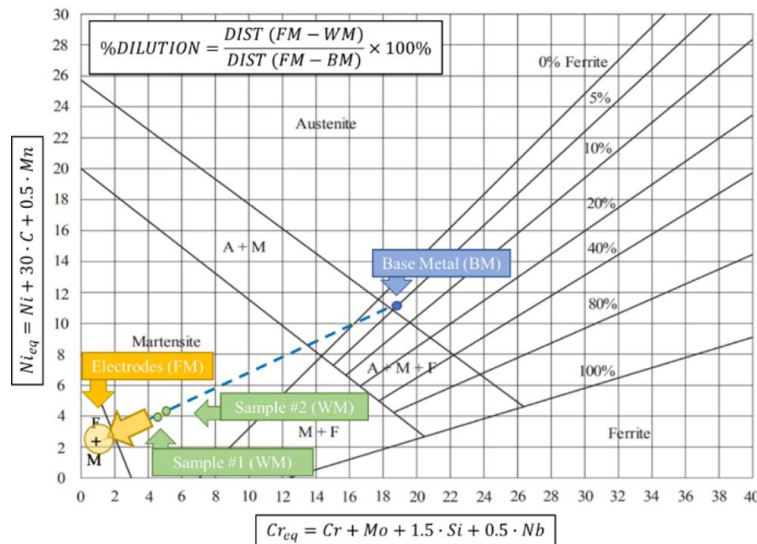


Figure 5. Schaeffler diagram with the average result of Type 316L steels (Base Metal), weld metals (Sample #1 and #2) and the composition of the family of filler metals (Electrodes).

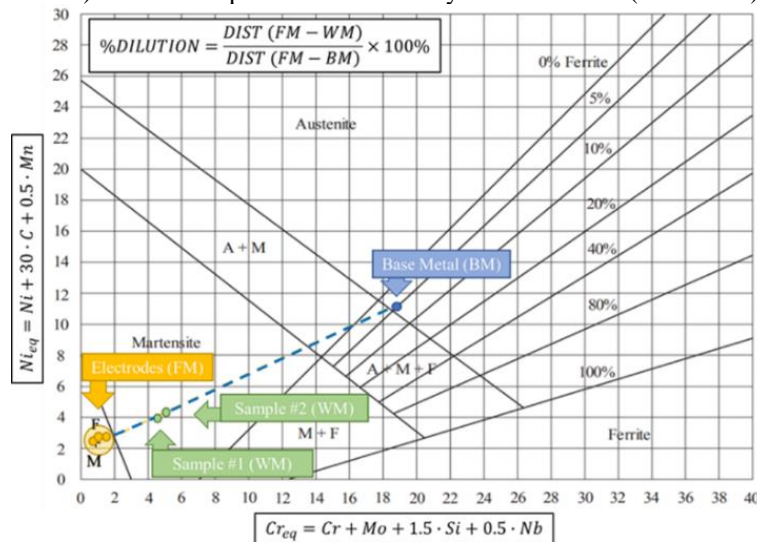


Figure 6. Schaeffler diagram with: Base metal Type 316L, weld metals (Samples #1 and #2) and the average of typical compositions of filler metals E7018 and ER70S-6.

Table 3. Creq and Nieq for two typical carbon-steel electrodes used in the Schaeffler and WRC-92 diagram

| ELECTRODE DESIGNATION                  | BRAND   | TYPICAL CHEMICAL COMPOSITION (% P/P) |      |      |       |      |      |      | SCHAEFFLER          |                     | WRC-92              |                     |
|--|---------|--------------------------------------|------|------|-------|------|------|------|---------------------|---------------------|---------------------|---------------------|
|  |         | C                                    | Cr   | Mn   | Mo    | P    | S    | Si   | Ni <sub>EQUIV</sub> | Cr <sub>EQUIV</sub> | Ni <sub>EQUIV</sub> | Cr <sub>EQUIV</sub> |
| AWS A5.1<br>STANDARD CLASS<br>E7018    | CONARCO | 0,08                                 |      | 1,25 |       |      |      | 0,45 | 3,0                 | 0,7                 | 2,8                 | 0,0                 |
|  | HARRIS  | 0,08                                 |      | 1,00 |       | 0,02 | 0,01 | 0,60 | 2,9                 | 0,9                 | 2,8                 | 0,0                 |
|  | INDURA  | 0,06                                 |      | 1,05 |       | 0,02 | 0,01 | 0,49 | 2,3                 | 0,7                 | 2,1                 | 0,0                 |
|  | LINCOLN | 0,05                                 |      | 1,00 |       | 0,02 | 0,01 | 0,30 | 2,0                 | 0,5                 | 1,8                 | 0,0                 |
| AWS A5.18<br>STANDARD CLASS<br>ER70S-6 | CARBONE | 0,07                                 |      | 0,89 |       | 0,01 | 0,01 | 1,48 | 2,5                 | 2,2                 | 2,5                 | 0,0                 |
|  | ESAB    | 0,08                                 |      | 1,22 |       | 0,01 | 0,01 | 0,67 | 2,9                 | 1,0                 | 2,6                 | 0,0                 |
|  | INDURA  | 0,08                                 |      | 1,44 |       | 0,01 | 0,01 | 0,86 | 3,1                 | 1,3                 | 2,8                 | 0,0                 |
|  | LINCOLN | 0,08                                 | 0,03 | 1,45 | 0,002 | 0,01 | 0,01 | 0,84 | 3,1                 | 1,3                 | 2,8                 | 0,0                 |
| AVERAGE FOR E7018:                     |         |                                      |      |      |       |      |      |      | 2,6                 | 0,7                 | 2,4                 | 0,0                 |
| STANDARD DEVIATION FOR E7018:          |         |                                      |      |      |       |      |      |      | 0,5                 | 0,2                 | 0,5                 | 0,0                 |
| AVERAGE FOR THE ER70S-6:               |         |                                      |      |      |       |      |      |      | 2,9                 | 1,5                 | 2,7                 | 0,0                 |
| STANDARD DEVIATION FOR E7018:          |         |                                      |      |      |       |      |      |      | 0,3                 | 0,5                 | 0,2                 | 0,0                 |
| TOTAL AVERAGE:                         |         |                                      |      |      |       |      |      |      | 2,7                 | 1,1                 | 2,5                 | 0,0                 |
| STANDARD DEVIATION FOR E7018:          |         |                                      |      |      |       |      |      |      | 0,4                 | 0,5                 | 0,4                 | 0,0                 |

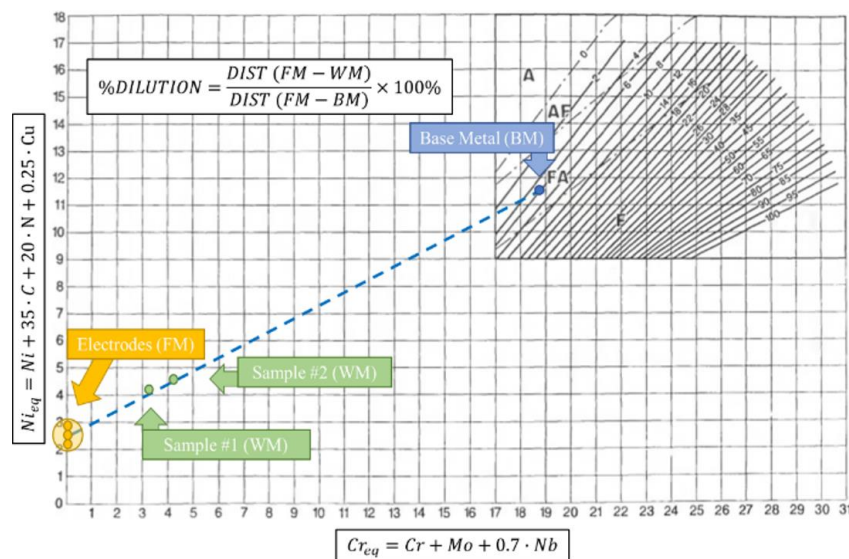


Figure 7. WRC-92 diagram with Type 316L steels (Base Metal), weld metals (Sample #1 and #2) and the standard composition of the electrodes E7018 and ER70S-6 (Electrodes).

The previous considerations, for instance the low chromium, nickel and molybdenum, and the galvanic effect due to the different weld metal composition of the weld metals which acts like an anode respect the base metal, explain the low corrosion resistance exhibited by the gate welds and its high magnetic attraction ( $FN > 80$ ).

The graphical representation of the weld metals (Samples #1 and #2) and the base metal from the gates in both constitution diagrams, Schaeffler and WRC-92, in conjunction with the average representation of typical filler metals E7018 or ER70S-6 from different brands, allow to affirm that the gates were welded with

classifications of filler metals belonging to carbon steel family such as those included in AWS A5.1 or 5.18 standards. The dilution calculated from both diagrams (20-23%) is characteristics of fillet weld dilutions.

The results suggest that an incorrect carbon steel filler metal was used during the construction of the austenitic stainless steel gates due to an inadequate WPS, a bad quality control system or, in the worst case, an attempt to save money by employing a carbon steel filler metal instead of an austenitic stainless steel.



#### 4. Conclusions

The weld metals in the gates could not be obtained with GMAW process using an ER316LSi filler metal as is established in the production WPS for the sliding gates given by the manufacturer.

The low corrosion resistance of the welds under atmospheric corrosion also showed that the welds were applied using an incorrect filler metal during the manufacture of the gates.

The chemical composition, microstructure, magnetic properties and hardness of the weld metals showed that the filler metals used during manufacturing were carbon steels, probably those included in AWS A5.1 or A5.18 standards such as E7018 or ER70S-6.

#### Acknowledgements

The authors would like to thank to Universidad Nacional de Colombia, Medellín, and the Instituto Tecnológico Metropolitano for their support and infrastructure, which enabled to develop this analysis.

#### References

- [1] A. M. El-Sherik, *Trends in oil and gas corrosion research and technologies: Production and transmission*, Cambridge, MA, USA: Woodhead Publishing, 2017.
- [2] E. D. Mackey and T. F. Seacord, "Guidelines for using stainless steel in the water and desalination industries," *J. Am. Water Works Assoc.*, vol. 109, no. 5, pp. E158–E169, 2017.
- [3] E. Mackey, T. Seacord, and S. Lamb, "Stainless Steel: How Problems Arise and How to Avoid Them," *Opflow*, vol. 39, no. 11, pp. 20–23, Nov. 2013, doi: 10.5991/OPF.2013.39.0068
- [4] *Fabricated stainless steel slide gates*, American Water Works Association, ANSI AWWA C561-04, 2004.
- [5] American Welding Society, *AWS D1.1/1.1M Structural Welding Code - Stainless steel*. Miami, FL; USA: 2004.
- [6] American Welding Society, *AWS A5.9/A5.9M Specification for Bare Stainless Steel Welding Electrodes and Rods*, Miami, FL; USA: AWS, 2012.
- [7] *Standard Specification for Chromium and Chromium-Nickel Stainless Steel Plate, Sheet, and Strip for Pressure Vessels and for General Applications*, ASTM A240, 2018.
- [8] H. Granjon, *Fundamentals of welding metallurgy*. Abington, PA; USA: Elsevier, 1991.
- [9] J. C. Lippold & D. J. Kotecki, *Welding metallurgy and weldability of stainless steels*. John Wiley & Sons Incorporated, 2005.
- [10] J.C Lippold, *Welding metallurgy and weldability*. Cambridge, Reino Unid: Woodhead, 2015.
- [11] Z. Zhang y R. A Farrar, *Atlas of continuous cooling transformation (CCT.) diagrams applicable to low carbon low alloy weld metals*. Cambridge, Reino Unido: Woodhead, 1995.
- [12] ASM International, *Welding, Brazing, and Soldering*. USA: ASM Handbook volume 6, 1993.
- [13] American Welding Society, *AWS A5.1/A5.1M: specification for carbon steel electrodes for shielded metal arc welding*. AWS USA: AWS, 2012.
- [14] American Welding Society, *AWS A5.18/A5.18M, Specification for Carbon Steel Electrodes and Rods for Gas Shielded Arc Welding*, USA: AWS, 2005.
- [15] S. Kou, *Welding metallurgy*. New Jersey, USA: Cambridge, 2003.
- [16] CONARCO, "Catálogo de Productos CONARCO ESAB para ferreterías," 2014. [Online]. Available: <http://cdechaco.com.ar/wp-content/uploads/2016/03/ESAB-CONARCO-Cat%C3%A1logo-Ferreter%C3%ADas.pdf>
- [17] TDS, "Technical specification sheet: E7018 covered electrode," Lawson Products, 2013. [Online]. Available: [https://www.lawsonproducts.com/pdfs/TDSWE\\_7018\\_Electrode\\_TS.pdf](https://www.lawsonproducts.com/pdfs/TDSWE_7018_Electrode_TS.pdf)
- [18] Welding consumables, (A-17 – B-3). Lincoln electric, 2017. [Online]. Available: <https://www.lincolnelectric.com/assets/EU/EN/consumables-catalogue-eng.pdf>